IRIS RECOGNITION BASED ON GAUSSIAN-HERMITE MOMENTS

Pravin .S.Patil

North Maharashtra University .
Jalgaon (M.S) India.
E-mail – pspatil777@gmail.com

Abstract. **Iris recognition is accepted as one of the most efficient biometric method. Implementing this method to the practical system requires the special image preprocessing where the iris feature extraction plays a crucial role. In this paper we have presented a new approach for iris feature extraction based on Gaussian-Hermite Moments. In the implemented algorithm, iris image is initially located by using circular contour method. Furthermore, intensity normalized flat bed iris image is generated by using Dougman's rubber sheet model, which is decomposed into a set of 1D intensity signals which retain most local variations of the iris, and then important and meaningful features have been extracted from such signals using Gaussian-Hermite Moments. Euclidian distance is used to measure the degree of dissimilarity between the iris feature vector sets. The recognition performance of the implemented algorithm has been observed. Experimental results show that the algorithm is efficient to describe local information. A CASIA iris database of iris images has been used for implementation.**

I. INTRODUCTION

In our modern networked society, with increasing demands of security, the technologies for personal identification work as main solution to safeguard people's properties.[1][2][3] Especially nowadays Security of computer and financial systems plays very significant role.[3] These systems require remembering many secrete code or passwords that may be forgotten even stolen or can be cracked by intercepting the presentation, or even by counterfeiting it.[4] In the second case results are usually disastrous for the user. In that case, biometrics becomes an alternative recognition technique in aspect of protecting ourselves. Biomertics employs physiological or behavioral characteristics to accurately identify each subject Commonly features include face, fingerprints, voice, iris retina and hand geometry etc.[1][2] Among all biometric iris recognition, is most reliable one.[5] Human Iris is a biometric that offers premium performance. Its strength lies in the rich unique textural information contained in the underlying tissues, Which is complex enough to be used as a biometric

signature.[6] These textural patterns are unique to each eye of an individual and even distinct between twins..Compared with other biometric features such as face and fingerprint; iris patterns are more stable and reliable. It is unique to people and stable with age [7][8]. Furthermore, iris recognition systems can be non-invasive to their users [7][8].

In order to implement iris recognition system the basic steps involved have been shown in Figure.1. To capture the details of the iris patterns, an imaging system should resolve a higher resolution iris scanner. Typically Monochrome CCD cameras are suitable most of the times. After capturing the eye image, the different kinds of operations need to be performed, which defines the IRIS recognition system.

The various steps involved in the iris recognition system can be well explained as 1) Iris image preprocessing 2) Iris feature extraction and 3) Iris feature matching In this paper we used circular contour method [13] to localize iris region. So far, various algorithms for iris recognition have been presented [9],[10],[11],[12]. Daugman [9], using phased-based approach, and by Boles et al. [10], where wavelet transform zero-crossing are used. Li Ma et al. [11][12], using Gabor filter and bank of Spatial filters.
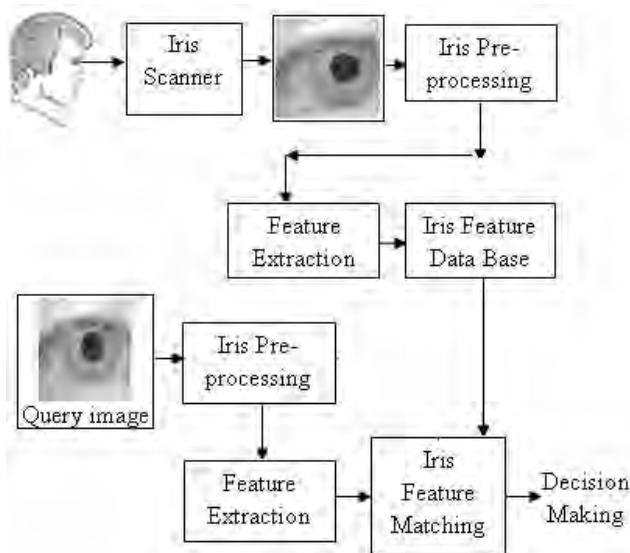
.Figure 1. Iris recognition system flow diagram.

Here, we develop a new approach based on Goussian-Hermite moment The remainder of this paper is organized as follows. Section II describes iris image preprocessing, which involves iris localization, iris normalization and image enhancement. Basic principles of iris feature extraction using Gaussian-Hermit moment are reviewed in detail in Section III Section IV introduces computation of feature vector Section V and Section VI gives the experimental results and conclusion.

II.   IRIS IMAGE PREPROCESSING

A. CIRCULAR IRIS LOCALIZATION USING RANDOM CIRCULAR CONTOUR METHOD

Step:1 A circular pseudo image is formed of the desired diameter.The diameter selected empirically in such way that, the circular contour will encircle the entire iris. The inside region of the circle is set at gray level '1'(white) and the outside region to '0'(black)

Step:2.This circular pseudo image is then convolved with the eye image from the database. It is partial localized iris image. The product of the gray levels of the circular pseudo image and the original have been illustrated in Figure.2(b).

(a)   (b)
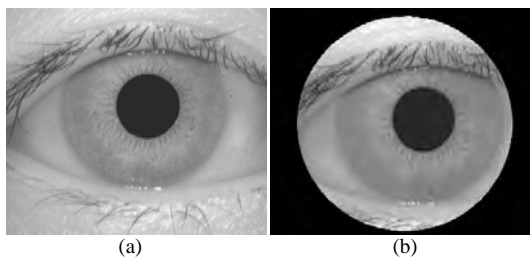
Figure 2.Formation of random circular contour around the iris (a) original eye in CASIA database (01_1_2.bmp), (b) marked random circular contour.

Step:3 To determine the pupilary center, we have used point image processing techniques such as thresholding and gray-level slicing (without the background),Which eliminate the other features of eye except the pupil of the eye. The pupil of the eye is set at gray level '0' (black) and rest of the region is set at '255' (white). The resultant pupil image has been illustrated in Figure.3

Step:4 Knowing the center of the frame and the center of the circular contour, the difference in the two centers can be determined.
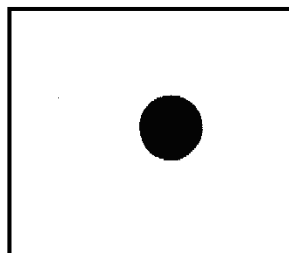
Figure 3. Pupil Image of the random circular contour around the iris

Using this difference, gray level shifting on the image has been carried out appropriately. The resultant image will have the center of the circular contour coinciding with the center of the frame. This has been illustrated in Figure.4.
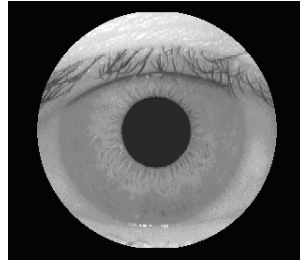
Figure 4 Centrally shifted random circular contour around the iris .

Step:5 In order to determine the limbus diameter we have used image point processing operators, mainly gray level slicing with and without the background and a digital negative, we obtain only the iris at gray level '0' (black) and the remaining portion of the image is at gray level '255' (white) . The shape of the limbus in this case can be considered to be semi-circular as shown in Figure 5.

Figure 5 Semi-circular limbus after gray level slicing.

Step:6 Finally, the result of iris localization of the eye with iris (limbus) and pupil are circled correctly in the aligned iris image has been demonstrated in Figure.6.
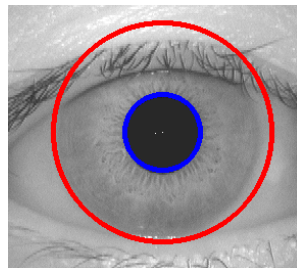
Figure 6.Aligned Iris in eye marked with circles for iris and pupil boundaries.

Step:7 Removing the portion of the iris occluded by the eyelids / eyelashes (as can be clearly observed from Figure.6) is very important because it affects the recognition results.[14] This is achieved by changing the gray level above the upper eyelids and below the lower eyelids to '0' (black).The resultant iris image after removal of the eyelids / eyelashes has been presented in Figure 10.
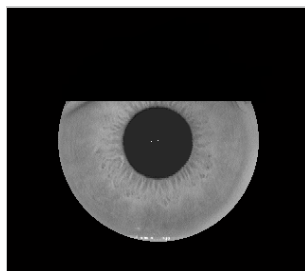
Figure 7 Resultant iris after removal of the eyelids / eyelashes.

B. FLAT BED IRIS LOCALIZATION

Irises from different people may be captured in different size and, even for irises from the same eye, the size may change due to illumination variations and other factors. such elastic deformation in iris texture will affects the results of iris matching.[12] The dimensional inconsistencies between eye images are mainly due to the stretching of the iris caused by pupil dilation from varying levels of illumination. Other sources of inconsistency include, varying imaging distance, rotation of the camera, head tilt, and rotation of the eye within the eye socket.[12] Another point of note is that the pupil region is not always concentric within the iris region, and is usually slightly nasal.[7] Daugman solved this problem[7][9][15].Flat bed iris localization is nothing but unwrapping the circular localized iris into a rectangular region using simple trigonometry. Image processing of the iris region is computationally expensive. In addition the area of interest in the image is a 'donut' shape, and grabbing pixels in this region requires repeated rectangular-to-polar conversions. [16][17] This allows the iris decoding algorithm to address pixels in simple (row, column) format. and to transform the iris region so that it has fixed dimensions in order to allow comparisons. Figure.8 shows simple implementation of the iris unwrapping.

The homogenous rubber sheet model can be shown in relevant to iris and pupil inside it. We can remap each point within the iris region to a pair of polar coordinates (r, θ) where r is on the interval [0, 1] and θ is the angle between [0, 2π].
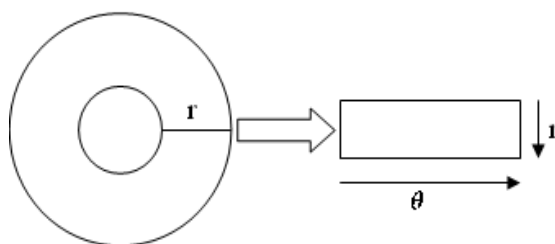
Figure 8. Implementation of iris unwrapping

The remapping of the iris region from (x, y) Cartesian coordinates to the normalized non-concentric polar representation is modeled as,

$$I(x(r,\theta), y(r,\theta)) \rightarrow I(r,\theta) \qquad (1)$$

with

$$x(r,\theta) = (1-r)\, x_p(\theta) + r\, x_1(\theta) \qquad (2)$$

$$y(r,\theta) = (1-r)\, y_p(\theta) + r\, y_1(\theta) \qquad (3)$$

where,

$\qquad$ $I(x, y)$ is the iris region image,

$\qquad$ (x, y) are the original Cartesian coordinates,

$\qquad$ (r, θ) are the corresponding normalized polar coordinates,

$\qquad$ x_p, y_p are the coordinates of the pupil, and

$\qquad$ x_1, y_1 are the iris boundaries along the θ direction.

 Even though the homogenous rubber sheet model accounts for pupil dilation, imaging distance and non-concentric pupil displacement, it does not compensate for rotational inconsistencies.

This procedure of iris unwrapping is applied on iris images from the CASIA V1 iris database and the resultant output has been illustrated in Figure 9.

(a) $\qquad\qquad\qquad\qquad\qquad$ (b)
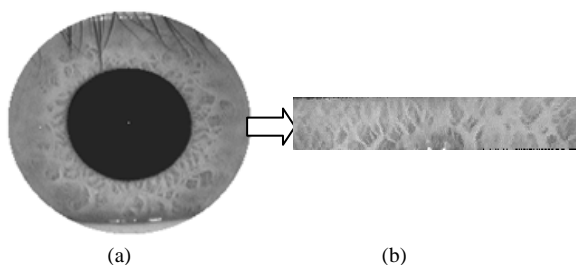
Figure 9 Flat bed iris localization (a) circular localized iris (CASIA V$_1$: 33_1_3.bmp), (b) Unwrapped normalize image.

In the experiments for generating the normalized flat bed iris image, we find that the iris region closer to the pupil provides the most discriminating information for recognition and is also rarely occluded by eyelids and

eyelashes. So we extract the flat bed iris for the region closer to the pupil as illustrated in Figure.10. This region takes up about 80% of the normalized image.
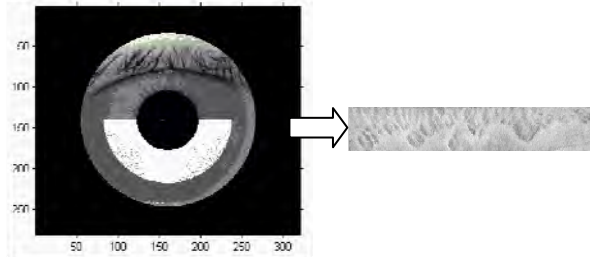
Figure 10. Extraction of flat bed iris for the region closer to the pupil.

The unwrapped normalized iris image still has low contrast and may have non-uniform brightness caused by the position of light sources.[12] In order to obtain a better distributed texture in the iris, we first approximate intensity variations across the whole iris image. The mean of each small block (we have considered the size of each block as 16×16 empirically) constitutes a coarse estimate of the background illumination. This estimate is further expanded to the same size as that of the normalized image by using bi-cubic interpolation. The resultant estimated background illumination for the same unwrapped normalized iris image has been illustrated in Figure.11.

Figure 11 Estimated background illumination.

This estimated background illumination is subtracted from the unwrapped normalized image to compensate for a variety of lighting conditions. Then we enhance the lighting corrected image by means of histogram equalization in each (32×32) region. Such processing compensates for non-uniform illumination, as well as improving the contrast of the image. Figure.12 shows the preprocessing result of an iris image, from which we can see that finer texture characteristics of the iris become clear.
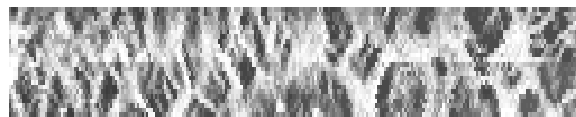
Figure 12. Enhanced unwrapped iris image.

III. IRIS FEATURE EXTRACTION USING GAUSSIAN-HERMITE MOMENTS
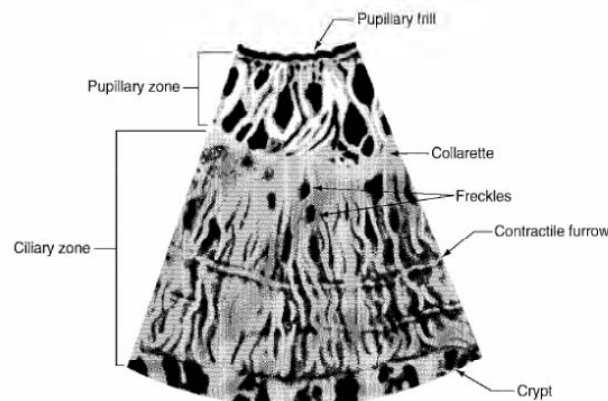
Figure 13. The complex pattern of Iris

Insightful observations about iris images from CASIA V_1 database [24] shows that iris complex pattern contain(figure.13) many distinctive features such as arching ligaments, furrows, ridges, crypts, rings, corona, freckles, and a zigzag collarets. That can be considered as elementary components of the iris texture. Colleratte area [18][19] as one of the most important parts of iris complex patterns, since it is usually less sensitive to the pupil dilation and less affected by the eyelids and eyelashes. This shape information provides the discriminating features for iris recognition. But these shapes are smaller in size so it is difficult to extract the edge information out of these shapes. Therefore we found that these irregular blocks cause noticeable local intensity variations in the iris images.[20] We approximately reflect shape information of the iris characteristics by analyzing the

resulting local variations in the iris image. In gray images, local intensity variations in the boundary of a region are generally sharper than those in the inside of a region.

Therefore, we expect to approximately reflect shape information of the iris blocks by analyzing local variations of the intensity signals. In this Section we have implemented the algorithm for iris recognition using Gaussian-Hermite Moments. In this algorithm a normalized image is first decomposed into a set of 1D intensity signals which retain most local variations of the iris, and then important and meaningful features have been extracted from such signals using Gaussian-Hermite Moments.

A. GENERATION OF 1D INTENSITY SIGNALS

Generally, local details of the iris spread along the radial direction in the original image corresponding to the vertical direction in the intensity normalized iris image. Therefore, information density in the angular direction corresponding to the horizontal direction in the normalized image is much higher than that in other directions. This can be easily observed in Figure 14. in which we have generated four 1-D signals corresponding to gray level intensity plots of four rows for intensity normalized flat bed iris image (from CASIA V_1 database)
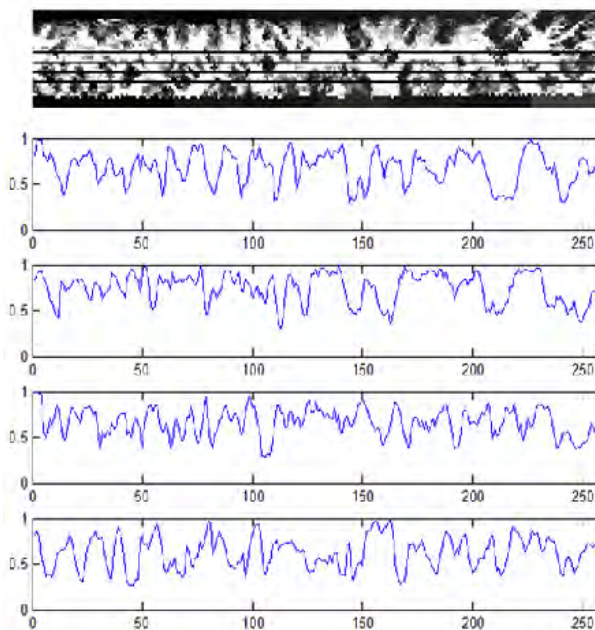
Figure 14 Generation of 1-D signals and there corresponding intensity plot of intensity normalized flat bed iris image from CASIA V_1 database (CASIA V_1: 13_1_3).

The information density in the angular direction corresponding to the horizontal direction in the normalized flat bed iris image is much higher than that in other directions. In addition, since the basic idea here is to reflect the shape information of the randomly distributed blocks or shapes for analyzing the local variations in the iris image in the selected rows of the flat bed iris image, it is unnecessary to capture local variations in every line of the iris flat bed image for recognition. Bearing these two points in mind, we decompose the 2-D normalized image into a set of 1D intensity signals by using,

$$S_i = \frac{1}{M}\sum_{j=1}^{M} I_{(i-1)} * (M + j), \ \ for \ i = 1,2,...,N \quad (4)$$

where,

$$I = \begin{pmatrix} I_1 \\ I_2 \\ . \\ . \\ I_x \\ . \\ . \\ I_K \end{pmatrix} = (I_1^T, I_2^T, ..., I_x^T, ..., I_K^T)^T \quad (5)$$

where,

I_x Denotes gray values of the xth row in the normalized flat bed iris image I of ($K \times L$),

M is the number of rows used to form a signal S_i and

N is the total number of 1-D signal.

In our experimentations we have used the normalized flat bed iris image I of size 64×256. Each signal S_i is the average of the M successively horizontal scan lines which reflects the local variations of the objects or shapes along the horizontal direction of the flat iris bed. The set of such signals should contain the majority of the local variations of the flat bed iris image. Such processing reduces the computational cost required for the subsequent feature representation. Thus the selection of number of rows, (a constant M) plays an important role in adjusting tradeoff between accuracy and speed of the implemented algorithm. A small value M leads to a large set of signals, which results in characterizing the iris details more completely, and thus increases recognition accuracy but increases the computational complexity. A large M, however, implies a lower recognition rate with a higher computational efficiency. For our experimentations we have selected value of M as 10 empirically. In the experiments for generating the normalized flat bed iris image, we find that the iris region closer to the pupil provides the most discriminating information for recognition also rarely occluded by eyelids and eyelashes. So we extract features only in the region closer to the pupil as explained in section II. This region takes up about 80% of the normalized image.

The generated four 1-D signals corresponding to gray level intensity plots of four rows for another normalized flat bed iris image from CASIA V_1 database have been illustrated in Figure.15 for comparison and understanding.
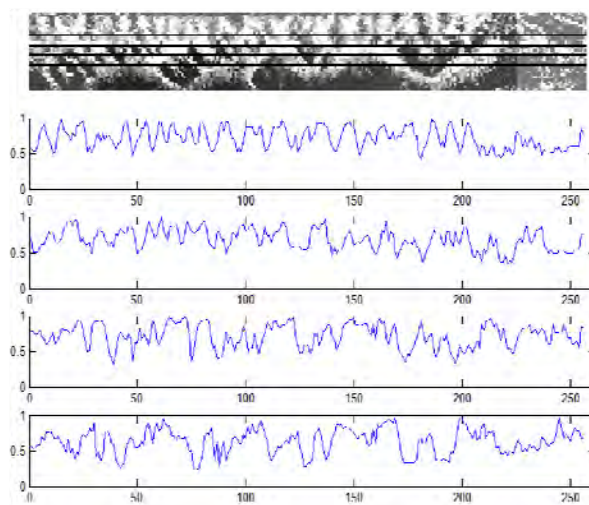
Figure 15 Generation of 1-D signals and there corresponding intensity plot another normalized flat bed iris image from CASIA V_1 database (CASIA V_1: 20_1_3).

B. GAUSSIAN–HERMITE MOMENTS

 Moment-based method has been widely used to represent local characteristics of images in pattern recognition and image processing. especially in various shape-based applications. The orthogonal moments, (as compared to traditional geometric moments) use orthogonal polynomial functions such as transform kernels, which produces minimal information redundancy.[21] In this algorithm Gaussian–Hermite moments have been used for feature extraction due to their mathematical orthogonality and effectiveness for characterizing local details of the signal.

The nth order 1-D Gaussian–Hermite moment $M_n(x)$ of a signal $S(x)$ is defined as,

$$M_n(x) = \int_{-\infty}^{\infty} K_n(t)S(x+t)dt, \quad for \; n = 0,1,2, \dots$$

(6)

where,

$$K_n(t) = g(t,\sigma)H_n\left(t/\sigma\right), \text{ and}$$

$$H_n(t) = (-1)^n exp(t^2)\frac{d^n\exp(-t^2)}{dt^n},$$

where,

$g(t,\sigma)$ is a Gaussian function,

$H_n(t)$ is a nth order Hermite polynomial function, and

$K_n(t)$ is the kernel that is a product of these two functions.
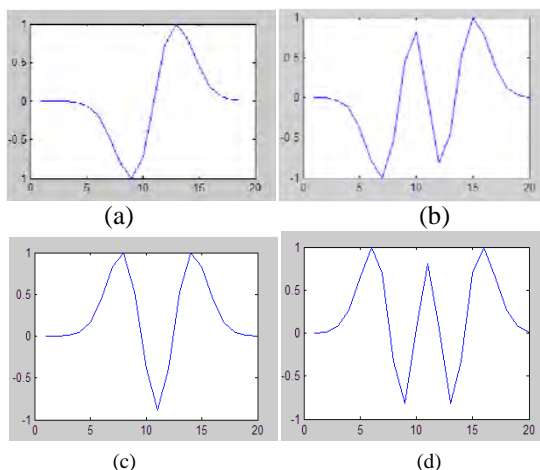
Figure 16 Gaussian–Hermite Moment kernels at various orders (a) 1st order kernel,

(b) 2nd order kernel, (c) 3rd order kernel, (d) 4th order kernel.

The Gaussian–Hermite moment kernels of various orders can be computed using (6). Figure 16 shows the spatial responses of the Gaussian–Hermite moment kernels of first four orders which we have used during our experimentations. The space constant of the Gaussian function in (6) affects the shape of the Gaussian–Hermite moment kernels. For our experimentations we have set the value of the space constant of the Gaussian function to 2.5 empirically. From the Figure 16 we can see that with the increase of the order of the moment kernels, oscillations of the moment kernels also increase. This implies that the moment kernels of different orders characterize different spatial modes. In fact, Gaussian–Hermite moments are linear combinations of the different order derivatives of a signal filtered by a Gaussian filter. The derivatives have been extensively used for image representation in pattern recognition. Here, our purpose is to analyze local variations of the resulting intensity signals. Gaussian–Hermite moments can well represent different spatial modes and are thus capable of effectively characterizing the differences between 1D intensity signals.[20][22] Moreover, from the viewpoint of spectral analysis, each moment kernel is somewhat similar to a band pass filter. The higher the moment kernel's order is, the higher its spatial frequency. This means that Gaussian–Hermite moments capture signal features over a broad frequency range. These desirable characteristics exhibited by Gaussian–Hermite moments make them a suitable choice for analyzing local variations of the intensity signals

IV. COMPUTATION OF FEATURE VECTOR

For each signal S_i, we can calculate its Gaussian–Hermite moment $M_{i,n}$ of the order n and i number of rows. In our experimentation work, we have generated 10 intensity signals, i.e. $i \in \{1,2,...,10\}$, and used 4 different order Gaussian –Hermite moments, i.e, $n \in \{1,2,3,4\}$. The space constant of the Gaussian function that affects the shape of the Gaussian–Hermite moment kernels has been set to 2.5. Since the outputs $M_{i,n}$ denote different local features derived using different moment kernels, we concatenate all these features together to form an integrated feature vector as,

$$V = \left(M_{1,1}, M_{1,2}, ..., M_{10,3}, M_{10,4}\right)^T \qquad (7)$$

where,

T is the transpose operator.

The length of each intensity signal is 256, since we have used the flat bed iris of 256 horizontal lengths; the feature vector V includes 10,240 (256×10×4) components. This feature map of all the template iris images has been computed and stored in the database. The feature map of a query iris image is then computed and this query feature map has been compared with the feature maps of template iris images in the database to find a correct match using Euclidian distance.[23] The Euclidian distance between trainee and query flat bed normalized iris image is given by,

$$d = \sum_{i=1}^{10} \sum_{n=1}^{4} \left(V - V'\right)^2 \qquad (8)$$

where,

V is the feature map of the trainee flat bed normalized iris image,

V' is the feature map of the query flat bed normalized iris image.

V.   EXPERIMENTS AND RESULTS

The algorithm has been implemented and tested on Pentium-IV processor with 2.6 GHz, 512 MB RAM under MATLAB environment. The standard database of CASIA V_1 has been used to perform the recognition experimentation work. Initially all the iris images from the database have been converted to flat bed intensity normalized iris images as explained in Section II (B)   Then using (4) to (7) we have computed the feature vectors of these entire flat bed normalized iris images and stored them in the database. When a query iris image is presented the feature vector of the query image is computed in the same way and it is matched with all the feature vectors of template iris images in the database using (8). The percentage recognition rate observed as 96.33%.
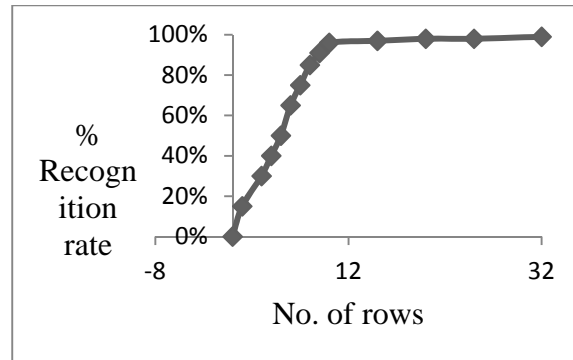
Figure 17 Plot of percentage recognition rate versus number of rows containing local intensity variations.

VI.   CONCLUSIONS

It has been observed that a set of one-dimensional (1-D) intensity variation signal is reflect effectively local shape information of two-dimensional (2-D) iris image. We have performed another experiment to find minimum number of rows used to compute the local intensity variations. For this purpose we have varied number of rows from 1 to 32 and the percentage recognition rate have been observed, which has been plotted in Figure17 The recognition performance of this algorithm founds to be 96.33% with ten rows of gray level local intensity variations. The performance elevates to 99.50% as the number of rows of gray level local intensity variations increases costing to computational complexity of the algorithm. It was notified during experimentation that as the number of rows has increased the computational time required for matching was very high.

VII .   REFERENCES

[1]   A.Jain and S.Pankanti, Biometric: Personal Identification in a networked society,   edsluswer, 1999
[2]   D.Zhang,Automated Biometrics: Technologies and   systems. Kluswer, 2000
[3]   .Daugman, "How iris recognition works," Proceeding of International conference on Image processing, vol. no.1, 2002.
[4]   Yong Wang and Jiu-Qiang Han "Iris Recognition Using Independent Component Analysis," Proceedings of the 4th International Conference on Machine Learning and Cybernatics, Gaungzhou, pp 4487-4492, 18-21 Aug. 2005
[5]   T.Mansfield, G.Kelly,D.Chandler ,and J.Kane, "Biometric product testing final report, issue   1.0", National Physical Laboratory of UK ,2001.
[6]   P.W. Hallinan, "Recognizing Human Eyes", *Geomtric Methods Computer Vision*, vol. 1570, pp.214-226,, 1991.
[7]   J.G. Daugman, "High Confidence Visual Recognition of Persons by a Test of Statistical Independence", *IEEE Transactions Pattern Analysis and Machine Intelligence*, vol.15, pp.1148-1161, Nov. 1993.
[8]   R.P. Wildes, "Iris Recognition: An Emerging Biometric Technology", *Proceedings of the IEEE,* vol.85, pp.1348-1363, Sept. 1997.
[9]   J.Daugman, "Statistical richness of visual phase information: Update on recognizing persons by iris patterns", International Journal of Computer Vision, Vol 45, No. 1, pp. 25-38, 2001.
[10]   W.W.Boles, "A security system based on Human iris identification using wavelet transform", Engineering Applications of Artificial Intelligence, Vol. 11, No. 1, pp. 77-85, 1998.
[11]   L.Ma, Y.H.Wang, T.N.Tan, "Iris recognition based on multichannel Gabor filtering". Proceedings of the Fifth AsianConference on Computer Vision (ACCV2002), Australia pp. 279-283, Jan. 2002.
[12]   Li Ma, Tieniu Tan, Yunhong Wang," Personal Identification Based on Iris Texture Analysis," IEEE transaction on Pattern analysis and machine intelligence, vol.25, no.12, pp 1519-1533, Dec. 2003.
[13]   N. Ritter, "Location of the pupil-iris border in slit-lamp images of the cornea," Proceedings of the International Conference on Image Analysis and Processing, 1999.
[14]   W. Kong, D. Zhang, "Accurate iris segmentation based on novel reflection and eyelashes detection model," Proceeding of 2001 International symposium on intelligent multimedia, video and speech processing Hong Kong, 2001.
[15]   J. Daugman, "Demodulation by Complex-Valued Wavelets for Stochastic Pattern Recognition," Int'l J. Wavelets, Multi-resolution and Information Processing, vol. 1, no. 1, pp 1-17, 2003.
[16]   Iris Recognition:Unwrapping the iris http://cnx.org/content/m12492/latest, 26/10/2006
[17]   Iris Recognition: Gabor filtering http://cnx.org/content/m12493/latest ,26/10/2006
[18]   R. Wildes "Iris recognition an emerging biometric technology," Proceeding of the IEEE, vol. 85, 1997.
[19]   H. Sung, J. Lim, Y. Lee, "Iris recognition using collarette boundary localization," Proceeding of the 17th International conference on pattern recognition, 2004
[20]   L.Ma,T.Tan,Y.Wang,D.Zhang " Local Intensity variation analysis for iris recognition,ELSEVIER Journal for Pattern recognition" vol 37 issue 6 pp 1287-1298

[21] Bo Yang and Mo Dai "Image analysis by Gaussian-Hemite moments.ELSEVIER Journal for signal processing" vol 91,issue 10 ,,pp 2290-2303 Oct 2011

[22] G. K.Viju N.K.,Salih,Tianyi Zang "A novel authentication" IEEE International Conference on Computer application and industrial Electronic,,pp-350-354,2011

[23] Y.Huang,S.Luo,and E.Chen,"An EfficientIrisRecognitionSystem,"proc.FirstInt'lconf.Machine Learning and Cybernetics,pp.450-454 Nov.2002

[24] " CASIA Iris Image Database", Institude of Chinese Academy of Sciences, http://www.sinobiometrics.com,2004

AUTHORS PROFILE

Mr. Pravin Sahebrao Patil holds Bachelor's degree in Electronics & Telecommunication from Marathwada University, Aurangabad (Maharashtra) in 1989 and Masters from Motilal Nehru National Institute of Technology at Allahabad in 1995. He join as research scholar in Dept. of Computer Sciences, North Maharashtra University from 2008. His area of interest is Digital image processing and communication system. Presently he is working as Associate Professor & Head in Dept.of Electronics & Communication at S.S.V.P.S's Bapusaheb .Shivajirao .Deore College of Engineering,Dhule,Maharashtra.